EUROPEAN ORGANISATION FOR NUCLEAR RESEARCH (CERN)

Submitted to: Eur. Phys. J. C

CERN-EP-2021-234
3rd December 2021

Search for flavour-changing neutral-current interactions of a top quark and a gluon in pp collisions at $\sqrt{s}$ = 13 TeV with the ATLAS detector

The ATLAS Collaboration

A search is presented for the production of a single top quark via left-handed flavour-changing neutral-current (FCNC) interactions of a top quark, a gluon and an up or charm quark. Two production processes are considered: $u + g \to t$ and $c + g \to t$. The analysis is based on proton–proton collision data taken at a centre-of-mass energy of 13 TeV with the ATLAS detector at the LHC. The data set corresponds to an integrated luminosity of 139 fb^{-1}. Events with exactly one electron or muon, exactly one b-tagged jet and missing transverse momentum are selected, resembling the decay products of a singly produced top quark. Neural networks based on kinematic variables differentiate between events from the two signal processes and events from background processes. The measured data are consistent with the background-only hypothesis, and limits are set on the production cross-sections of the signal processes: $\sigma(u + g \to t) \times \mathcal{B}(t \to Wb) \times \mathcal{B}(W \to \ell\nu) < 3.0$ pb and $\sigma(c + g \to t) \times \mathcal{B}(t \to Wb) \times \mathcal{B}(W \to \ell\nu) < 4.7$ pb at the 95% confidence level, with $\mathcal{B}(W \to \ell\nu) = 0.325$ being the sum of branching ratios of all three leptonic decay modes of the W boson. Based on the framework of an effective field theory, the cross-section limits are translated into limits on the strengths of the tug and tcg couplings occurring in the theory: $|C_{uG}^{ut}|/\Lambda^2 < 0.057\,\text{TeV}^{-2}$ and $|C_{uG}^{ct}|/\Lambda^2 < 0.14\,\text{TeV}^{-2}$. These bounds correspond to limits on the branching ratios of FCNC-induced top-quark decays: $\mathcal{B}(t \to u + g) < 0.61 \times 10^{-4}$ and $\mathcal{B}(t \to c + g) < 3.7 \times 10^{-4}$.

Contents

1 Introduction **2**

2 The ATLAS detector **4**

3 Samples of data and simulated events **5**
3.1 Samples of simulated events from the ugt and cgt FCNC processes 5
3.2 Simulation of $t\bar{t}$ and SM single-top-quark production 6
3.3 Simulation of W+jets and Z+jets production 7
3.4 Simulation of diboson and multijet production 7

4 Object reconstruction and event selection **8**
4.1 Object definitions 8
4.2 Basic event selection 9
4.3 Definition of signal and validation regions 10

5 Estimation of the multijet background **11**

6 Neural networks separating signal and background events **14**

7 Systematic uncertainties **17**
7.1 Experimental uncertainties 18
7.2 Modelling uncertainties 18

8 Results **20**
8.1 Results of the profile likelihood fit 21
8.2 Upper limits on cross-sections, EFT coefficients and branching ratios 24
8.3 Comparison of expected upper limits 25

9 Conclusions **26**

1 Introduction

Direct searches for on-shell production of new heavy particles at the Large Hadron Collider (LHC) have not yet been successful. For this reason, indirect searches targeting non-standard couplings among Standard Model (SM) particles attract increasing interest. Among these analyses are searches for flavour-changing neutral-current (FCNC) processes in the top-quark sector. The SM does not contain FCNC processes at tree level, and even though these processes exist at higher orders, they are suppressed due to the Glashow–Iliopoulous–Maiani mechanism [1]. Compared to the b-quark sector, where decays of b-hadrons via FCNCs were first observed in 1995 [2], FCNC decays of top quarks are even more suppressed. Depending on the decay mode, FCNC branching ratios ($\mathcal{B}$) of the top quark are predicted to range from 10^{-12} to 10^{-17} [3], and are thus well below the experimentally accessible regime, at present and in the foreseeable future. The observation of FCNC top-quark decays or top-quark production via FCNCs would therefore be an unambiguous signal of physics beyond the SM.

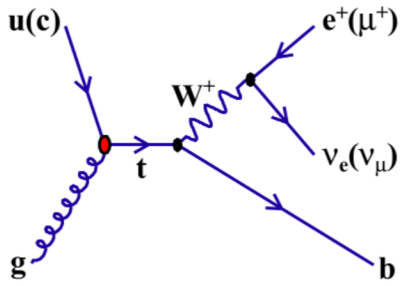

Figure 1: Leading-order Feynman diagram of non-SM production of a single top quark via the FCNC process $u(c) + g \to t$.

Many extensions of the SM predict significantly higher rates for FCNC processes in the top-quark sector. These extensions include new scalar particles introduced in two-Higgs-doublet models [4, 5] or in supersymmetry [6–8]. In certain regions of the parameter space of these models, the predicted FCNC branching ratios of top quarks can be as large as 10^{-5} to 10^{-3} and thus become detectable at the LHC.

Searches for FCNCs involving a top quark and a gluon were performed at the Tevatron [9, 10] and in data from Run 1 of the LHC [11–13]. Rather than looking for the top-quark decays $t \to u + g$ and $t \to c + g$ in top-quark–antiquark pair ($t\bar{t}$) production, these analyses searched for the production of a single top quark (t) via the FCNC processes $u + g \to t$ (ugt process) and $c + g \to t$ (cgt process), exploiting specific kinematic features of single-top-quark production to separate a potential signal from the large W+jets and multijet backgrounds. The analysis presented in this paper extends the Run 1 ATLAS search to the Run 2 data set collected with the ATLAS detector in the years 2015 to 2018, during which the LHC operated at a centre-of-mass energy of 13 TeV. Conceptually, the scope of the analysis is expanded by performing independently optimised searches for the ugt and cgt processes. Differences between these two processes are due to differences in the parton distribution functions (PDFs) for valence and sea quarks. For top antiquarks the charge-conjugate processes are implied. The FCNC interaction is assumed to be left-handed.

The event selection targets the $t \to e^+\nu b$ and $t \to \mu^+\nu b$ decay modes of the top quark. However, there is also additional but lower acceptance for events with the decay $t \to \tau^+\nu b$ and the subsequent decay of the τ-lepton into $e^+\nu_e\bar{\nu}_\tau$ or $\mu^+\nu_\mu\bar{\nu}_\tau$. A leading-order (LO) Feynman diagram illustrating the signature of the targeted scattering events is shown in Figure 1. Considering the signature of the signal events, the required reconstructed objects are exactly one charged-lepton candidate (an electron or a muon) with high transverse momentum (p_{T}), exactly one jet which is identified to originate with high probability from a b-quark, and large missing transverse momentum as an indication of a high-p_{T} neutrino.

The main background processes are $W + b\bar{b}$ production, t-channel single-top-quark (tq) production, and $t\bar{t}$ production. Artificial neural networks (NNs) are used to separate signal events from background events. The observed distributions of the NN discriminants are analysed statistically with a profile maximum-likelihood fit in which all systematic uncertainties are treated as nuisance parameters. The results are interpreted in an effective field theory framework provided by the `TopFCNC` model [14].

The structure of the paper is as follows. A brief description of the ATLAS detector is given in Section 2, followed by a comprehensive summary of the collision data and the samples of simulated events in Section 3. Section 4 describes the reconstruction of detector-level objects and the event selection. The modelling of

multijet background events and the estimation of their rate is discussed in Section 5. Section 6 provides details about the separation of signal and background events using NNs. Systematic uncertainties are outlined in Section 7 and the results are presented in Section 8. Conclusions are given in Section 9.

2 The ATLAS detector

The ATLAS detector [15] at the LHC covers nearly the entire solid angle around the collision point.[1] It consists of an inner tracking detector surrounded by a thin superconducting solenoid, electromagnetic and hadronic calorimeters, and a muon spectrometer incorporating three large superconducting toroidal magnets.

The inner-detector system (ID) is immersed in a 2 T axial magnetic field and provides charged-particle tracking in the range $|\eta| < 2.5$. The high-granularity silicon pixel detector covers the vertex region and typically provides four measurements per track, the first hit normally being in the insertable B-layer installed before Run 2 [16, 17]. It is followed by the silicon microstrip tracker, which usually provides eight measurements per track. These silicon detectors are complemented by the transition radiation tracker (TRT), which enables radially extended track reconstruction up to $|\eta| = 2.0$. The TRT also provides electron identification information based on the fraction of hits (typically 30 in total) above a higher energy-deposit threshold corresponding to transition radiation.

The calorimeter system covers the pseudorapidity range $|\eta| < 4.9$. Within the region $|\eta| < 3.2$, electromagnetic calorimetry is provided by barrel and endcap high-granularity lead/liquid-argon (LAr) calorimeters, with an additional thin LAr presampler covering $|\eta| < 1.8$ to correct for energy loss in material upstream of the calorimeters. Hadronic calorimetry is provided by the steel/scintillator-tile calorimeter, segmented into three barrel structures within $|\eta| < 1.7$, and two copper/LAr hadronic endcap calorimeters. The solid angle coverage is completed with forward copper/LAr and tungsten/LAr calorimeter modules optimised for electromagnetic and hadronic measurements respectively.

The muon spectrometer (MS) comprises separate trigger and high-precision tracking chambers measuring the deflection of muons in a magnetic field generated by superconducting air-core toroids. The field integral of the toroids ranges between 2.0 and 6.0 T m across most of the detector. A set of precision chambers covers the region $|\eta| < 2.7$ with three layers of monitored drift tubes, complemented by cathode-strip chambers in the forward region, where the background is highest. The muon trigger system covers the range $|\eta| < 2.4$ with resistive-plate chambers in the barrel, and thin-gap chambers in the endcap regions. Interesting events are selected to be recorded by the first-level trigger system implemented in custom hardware, followed by selections made by algorithms implemented in software in the high-level trigger [18]. The first-level trigger accepts events from the 40 MHz bunch crossings at a rate below 100 kHz, which the high-level trigger reduces in order to record events to disk at about 1 kHz.

An extensive software suite [19] is used in the reconstruction and analysis of real and simulated data, in detector operations, and in the trigger and data acquisition systems of the experiment.

[1] ATLAS uses a right-handed coordinate system with its origin at the nominal interaction point (IP) in the centre of the detector and the z-axis along the beam pipe. The x-axis points from the IP to the centre of the LHC ring, and the y-axis points upwards. Cylindrical coordinates (r, ϕ) are used in the transverse plane, ϕ being the azimuthal angle around the z-axis. The pseudorapidity is defined in terms of the polar angle θ as $\eta = -\ln\tan(\theta/2)$. Angular distance is measured in units of $\Delta R \equiv \sqrt{(\Delta\eta)^2 + (\Delta\phi)^2}$.

3 Samples of data and simulated events

The analysis uses proton–proton (pp) collision data recorded with the ATLAS detector in the years 2015 to 2018 at a centre-of-mass energy of 13 TeV. After applying data-quality requirements [20], the data set corresponds to an integrated luminosity of 139 fb^{-1} with a relative uncertainty of 1.7% [21]. The LUCID-2 detector [22] was used for the primary luminosity measurements. At the high instantaneous luminosity reached at the LHC, events were affected by additional inelastic pp collisions in the same and neighbouring bunch crossings (pile-up). The average number of interactions per bunch crossing was 33.7.

Events were selected online during data taking by single-electron or single-muon triggers [23, 24]. Multiple triggers were used to increase the selection efficiency. The lowest-threshold triggers utilised isolation requirements for reducing the trigger rate. The isolated-lepton triggers had p_{T} thresholds of 20 GeV for muons and 24 GeV for electrons in 2015 data, and 26 GeV for both lepton types in 2016, 2017 and 2018 data. They were complemented by other triggers with higher p_{T} thresholds but no isolation requirements in order to increase the trigger efficiency.

Large sets of simulated events from signal and background processes were produced with event generator programs based on the Monte Carlo (MC) method to model the recorded and selected data. After event generation, the response of the ATLAS detector was simulated using the GEANT4 toolkit [25] with a full detector model [26] or a fast simulation [27, 28] which employed a parameterisation of the calorimeter response. To account for pile-up effects, minimum-bias interactions were superimposed on the hard-scattering events and the resulting events were weighted to reproduce the observed pile-up distribution. The minimum-bias events were simulated using PYTHIA 8.186 [29] with the A3 [30] set of tuned parameters and the NNPDF2.3LO PDF set [31]. Finally, the simulated events were reconstructed using the same software as applied to the collision data. Except for the multijet background, the same event selection requirements were applied and the selected events were passed through the same analysis chain. Small corrections were applied to simulated events such that the lepton trigger and reconstruction efficiencies, jet energy calibration and b-tagging efficiency were in better agreement with the response observed in data. More details of the simulated event samples are provided in the following subsections.

3.1 Samples of simulated events from the ugt and cgt FCNC processes

Simulated events from the ugt and cgt processes were produced with the METOP 1.0 event generator [32, 33] at next-to-leading order (NLO) in quantum chromodynamics (QCD). The difference between LO and NLO is very relevant for the analysis since a veto on a second jet is applied in the event selection by requiring exactly one reconstructed jet with $p_{\text{T}} > 30$ GeV. The Lorentz structure of the vertex coupling was taken to be left-handed. It was verified that the shapes of kinematic distributions of both samples are independent of the values of the coupling constants used for the event generation. The top quark was assumed to decay as in the SM and the decay was simulated using MADSPIN [34, 35]. Only leptonic decays of the W boson originating from top-quark decay were considered, including $e^{\pm}$, $\mu^{\pm}$ and $\tau^{\pm}$ leptons. The renormalisation scale μ_{r} and the factorisation scale μ_{f} were set to the top-quark mass m_t, for which a value of $m_t = 172.5$ GeV was used. The CT10 set of PDFs [36] was used for event generation. Parton showers and the hadronisation were simulated with PYTHIA 8.235 [37] with the A14 set of tune parameters [38]. In the METOP+PYTHIA set-up, hard gluon emissions can arise in both the NLO matrix-element generator and the parton-shower generator. The matching between the two generators was achieved by limiting the phase-space region of the first parton-shower emission in a way that depends on the transverse momentum